ELSEVIER

Surface Science 377–379 (1997) 1–6

surface science

Ordering of vacancies on Si(001) [1]

H.J.W. Zandvliet

Faculty of Applied Physics and Centre of Materials Research, University of Twente, P.O. Box 217, 7500 AE Enschede, The Netherlands

Received 1 August 1996; accepted for publication 9 September 1996

Abstract

Missing dimer vacancies are always present on the clean Si(001) surface. The vacancy density can be increased by ion bombardment (Xe^+, Ar^+), etching (O_2, Br_2, I_2, etc.) or Ni contamination. The equilibrium shape at low vacancy concentrations (<0.2–0.3 monolayers) of these vacancy islands is elongated in a direction perpendicular to the dimer rows of the upper terrace, whereas for higher vacancy concentrations the equilibrium shape is rotated by 90°. The absence of dimerisation within the narrow vacancy islands at low vacancy concentration alone is not sufficient to explain this shape transformation, therefore it is suggested that the specific rebonding of these structures also plays a role. A more detailed analysis of the annealing behaviour, width, spacing between and depth of the elongated low-vacancy concentration vacancy islands reveals that the Ni-induced vacancy islands differ significantly from the etching-induced vacancy islands.

Keywords: Low index single crystal surfaces; Scanning tunneling microscopy; Self-assembly; Silicon; Surface energy; Surface stress; Surface thermodynamics

1. Introduction

Understanding the atomic structure of materials, the behaviour and reactions of atoms at surfaces and the nature of electronic properties at the atomic scale have been the goals of fundamental and applied research for many decades. The development of scanning tunnelling microscopy (STM) has revolutionised our approach to the investigation of many aspects of material properties at the atomic scale. Using STM, surface defects like steps, kinks, vacancies, etc. can now be studied on the atomic scale. These surface defects often play a key role in thin film growth processes. The Si(001) surface has, due to its technological importance, as well as its relatively simple structure, been a model system for several decades. In this paper I will focus on one type of surface defect of the Si(001) surface, namely missing dimer vacancies. It is well known that single and double missing-dimer vacancies are always present on the Si(001) surface. They are created during cleaning and a fair fraction survives after annealing. However, controlled amounts can be created by sputtering with noble gases (Xe^+, Ar^+) [1–3] or etching (O_2, Br_2, I_2, etc.) [4–6]. The motion of these relatively mobile vacancies [7] makes that, at elevated temperatures, they coalesce into vacancy islands. For low vacancy concentrations (<0.2–0.3 ML) and annealing at sufficiently high temperatures (>800 K) it turns out that the vacancy islands have their long axis aligned in a direction perpendicular to the dimer rows of the upper terrace [8]. At higher vacancy

[1] Invited paper.

PII S0039-6028(96)01316-7

concentrations, however, the vacancy islands have their long axis aligned along the dimer row direction of the upper terrace. At first sight (when the strain relaxation terms and reduction in dangling bonds or bonding distances are not taken into account) the appearance of the orientation where the vacancy islands are aligned perpendicular to the dimer rows of the upper terrace seems to be the opposite of what one should expect: the anisotropy of the nearest neighbour interaction between dimers, i.e. a strong interaction for neighbour dimers in the same row versus a much weaker interaction between neighbouring dimers in adjacent rows, should favour vacancy islands oriented with their long axis along the dimer rows. This puzzle is even more complicated because under specific (kinetic) conditions only vacancy islands elongated along the dimer rows are observed. At high supersaturation and relatively low temperatures, Bedrossian and Klitsner [1] observed only vacancy islands elongated along the dimer rows of the upper terrace. As has been correctly pointed out by these authors [1] there is a strong difference in the step edge retraction speed of the two different step edges on Si(001). The fact that the S_B edges retract faster than the S_A edges means that the vacancy island expands much faster along the dimer rows than perpendicular to the dimer rows. After thus having made plausible that the orientation of the vacancy islands which emerge during ion bombardment at moderate temperatures are controlled by kinetic effects it remains to be seen which vacancy island configuration represents (for a given vacancy concentration) the true equilibrium configuration. In the following I refer to the elongated vacancy islands oriented perpendicular to the dimer rows as vacancy line defects (VLD). The averaged spacing between the VLD is denoted L and the width of the VLD is denoted l. As already mentioned, small traces of metal (Ni or Cu) contamination gives rise to a similar looking VLD pattern [9]. The first real-space Ni-induced Si(001) images were reported by Niehus and co-workers [9]. The VLD network was found in their STM images at both positive and negative sample bias voltages, confirming the geometric origin of the VLD. Line scans across the Ni-induced VLD reveal that they are actually deeper than one atomic layer. There is currently, however, no evidence that the VLD defects induced by sputtering or etching are deeper than one atomic layer. Furthermore, there is another remarkable difference between the two different types of VLD: when the etched or sputtered surfaces are flash annealed for a few seconds at temperatures around 1500 K, the surfaces are completely restored without any trace of VLD, whereas the Ni-induced VLD cannot be annealed away [2]. The ordering of the missing-dimer vacancies into VLD is driven by an attractive interaction between vacancies in adjacent rows and a long-range repulsive interaction between the VLD. First, I will demonstrate that the long-range interaction decays as L^{-2} and is a consequence of surface strain relief. Second, it will be shown that the thermally-induced wandering of the various VLD displays universal behaviour and that the strength of this strain relaxation term can be extracted. Third, I will show that the absence of dimerisation within the vacancy island at low vacancy concentration alone cannot explain the equilibrium shape at low vacancy concentrations.

2. Experimental

The base pressure in the ultrahigh vacuum (UHV) chamber used during the scanning tunnelling microscopy experiments was $<1 \times 10^{-10}$ Torr. The Si(001) surfaces were cleaned by annealing the sample several times at 1500 K for several seconds followed by quenching to room temperature. During annealing, the chamber pressure did not rise above 2×10^{-9} Torr. After the annealing treatment, the sample was transferred to the scanning tunnelling microscope where the usual (2×1) reconstructed Si(001) surface was observed. The differentially pumped ion gun produced a beam of 3 keV Ar^+ ions incident normally onto the Si surface. The ion current, as measured with a Faraday cup, was adjusted to give various doses, ranging from 7×10^{11} to 6×10^{12} ions cm^{-2}. Typical ion currents used were 5 and 10 nA. After bombardment at room temperature, the sample was transferred back to the STM for atomically resolved imaging of the ion impacts on the surface. After imaging, the bombarded surfaces were

annealed for two minutes at temperatures ranging from 500–1500 K and imaged again. The Si samples were mounted on a Mo/Ta sample holder. Only one of the sample holders contained a single stainless steel screw mounted in the direct neighbourhood of the sample in order to introduce the Ni contamination. In this way the amount of Ni contamination increases slightly after each flash.

3. Results and discussion

Fig. 1 shows a Si(001) surface prior to the ion bombardment experiment (Fig. 1a), after room temperature bombardment by 3 keV Ar^+ ions at normal incidence with a dose of 1.5×10^{12} ions cm^{-2} (Fig. 1b) and the same surface after annealing for 2 min at 1025 K (Fig. 1c). After ion bombardment at room temperature the defect and adatom clusters are distributed randomly over the surface, whereas the vacancy clusters line up into VLD after the 2 min anneal at 1025 K [2]. Low-dose etching at elevated temperatures with various other gases, such as O_2 [5] and Br_2, I_2 [4], results in a similar VLD network. Line scans across these VLD reveal that they are probably not deeper than one atomic layer, i.e. 1.36 Å [10]. Although several "diluted" dimers can be observed in Fig. 1c their density turns out to be substantially lower as compared to the Ni-induced VLD (see Fig. 2). Fig. 2 shows a high-resolution STM image of a Ni-contaminated Si(001) surface. The average width of the VLD is about 2.5 dimer spacings and the depth, as measured with the STM, is about 1.9–2.0 Å. The most frequently appearing missing dimer configurations along the VLD are: a double missing dimer defect, a complex structure consisting of a double missing dimer defect and a single dimer defect separated by a single "diluted" dimer. These defect structures and other, rarer, configurations have also been identified by others [9,12,13,18]. The density of diluted dimers is about 5% of a monolayer, resulting in a Ni coverage of about 10% of a monolayer (using the estimate of Ukraintsev and Yates [18] that one diluted dimer

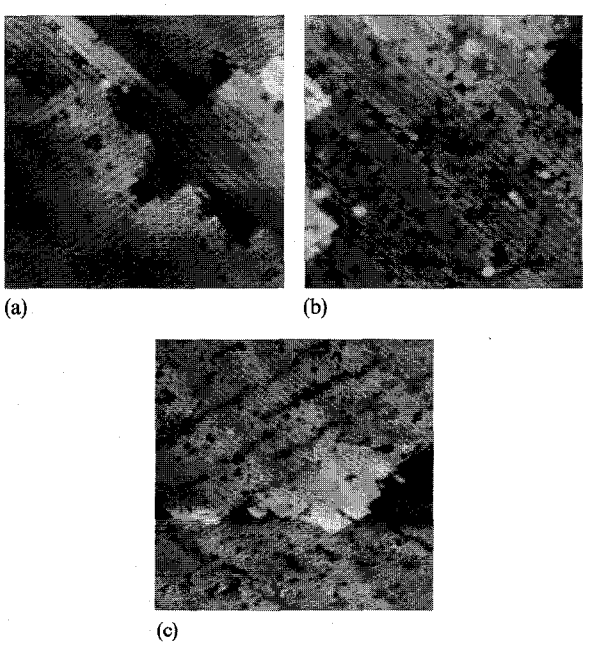

Fig. 1. (a) Clean Si(001) prior to ion bombardment. Sample bias is −2 V and tunnelling current is 0.5 nA. Scan area is 280 × 280 Å. (b) After bombardment by 3 keV Ar^+ ions at a dose of 1.5×10^{12} ions cm^{-2}. Sample bias is −2 V and tunnelling current is 0.5 nA. Scan area is 260 × 260 Å. (c) Bombarded surface after annealing at 1025 K for 2 min.

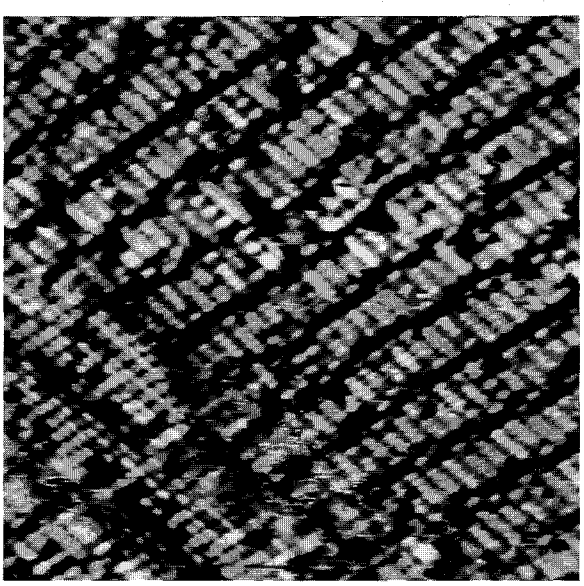

Fig. 2. High resolution STM image of a Ni (a few percent of a monolayer) contaminated Si(001) surface. The scan area is 250 × 250 Å, the sample bias −2 V and the tunnelling current 0.5 nA.

roughly corresponds to two Ni atoms). With increasing vacancy concentration the averaged width, l, of the VLD increases only marginally, whereas the averaged spacing between them, L, decreases much more rapidly. I will first compare these observations with a model, recently proposed by Zeppenfeld et al. [14]. The Zeppenfeld model is based on the energy balance between the creation of domain walls and the repulsive L^{-2} interaction between these walls. I consider here the quasi-one-dimensional (i.e. striped) domain structure. The energy, E, per unit length can, following Ref. [14], be written as:

$$E = E_{\text{boundary}} - E_{\text{strain-relaxation}} \tag{1a}$$

$$E_{\text{boundary}} = \frac{2\gamma}{l+L} \tag{1b}$$

$$E_{\text{strain-relaxation}} = \frac{2\sigma}{l+L} \ln\left[\frac{l+L}{2\pi a_0} \sin\left(\frac{\pi l}{l+L}\right)\right], \tag{1c}$$

where γ is associated with the creation of the domain boundaries between the minority domain of width l and the majority domain of width L. The term in Eq. (1c) describes the elastic relaxation: a_0 is a microscopic cutoff (e.g. the lattice constant) and σ is a function of the elastic constants and of the difference of the surface stress of upper terrace and lower terrace domain. In the case of *dimerisation* of both terraces and a monolayer deep vacancy island, σ can be written as:

$$\sigma = \frac{(\sigma_{\parallel} - \sigma_{\perp})^2(1-\nu)}{2\pi\mu} \tag{2}$$

where $\sigma_{\parallel}(\sigma_{\perp})$ refers to the intrinsic surface stress component along (perpendicular) to the dimer bond, μ to the bulk modulus of Si and ν to the Poisson's ratio of Si. Dimerisation within the vacancy island implies that the strain relaxation term, σ, is the same for both types of vacancy island edges. One should therefore expect that the vacancy islands have their long axis aligned along the lowest energy island edges, i.e. the S_A type edges. For high vacancy concentrations (typically >0.3 ML) created by ion bombardment at room temperature followed by annealing (the kinetic explanation mentioned earlier doesn't apply here), dimerisation within the vacancy island is indeed observed and these islands have their long axis aligned along the dimer rows of the upper terrace [5,6,11]. For lower vacancy concentrations there is, however, a shape transition to vacancy islands which have their long axis aligned in a direction perpendicular to the dimer rows of the upper terrace. Whether or not there is dimerisation within the VLD cannot be resolved with STM. Anyway, let us consider the low vacancy concentration case first in more detail. If the logarithmic term. In Eq. (1c) is expanded for small displacements δL around the minimum-energy configuration one finds that the leading term, which mimics the long-range interaction between the domain walls, is proportional to L^{-2}. From the minimalisation of the energy of surface systems governed by an effective long-range interactions decaying as L^{-2}, Zeppenfeld et al. found that, independent of the actual values of γ and σ, the following relation between the size of the minority domain l at a certain coverage $\theta = l/(L+l)$ and the minimal size of the minority at a coverage approaching zero, i.e. l_0, must hold;

$$l = l_0 \frac{\pi\theta}{\sin(\pi\theta)} \tag{3a}$$

$$l + L = l_0 \frac{\pi}{\sin(\pi\theta)}. \tag{3b}$$

In Fig. 3 a plot of the periodicity, $l+L$, of the Ni-induced and the Ar^+-induced pattern as well as the width, l, of the VLD in units of the dimer–dimer spacing versus coverage is shown. Because the Zeppenfeld et al. size relation is obeyed so well in the Ni-induced case we conclude that the VLD structure is indeed stabilised by an effective long-range interaction decaying as L^{-2}. The same plots of l and $l+L$ versus coverage for the etching-induced VLD reveal that in this case the Zeppenfeld model isn't obeyed that well. Among the differences are: a larger width, l, and significantly smaller chain lengths. This is most probably related to the fact that the etching-induced VLD

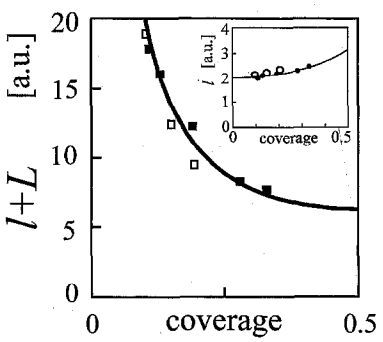

Fig. 3. Periodicity, $l+L$, in units of a (=3.84 Å) of the VLD pattern versus coverage ($=l/(l+L)$). Solid line: $l_0\pi/\sin(\pi\theta)$. Inset: width, l, in units of a of the VLD versus coverage. Solid line $l_0\pi\theta/\sin(\pi\theta)$. Filled squares and circles refer to Ni-induced VLD. Open squares and circles refer to Ar^+-induced VLD.

haven't, due to the lower anneal temperature, fully equilibrated.

In order to extract the exact strength of the long-range repulsive interaction between the VLD the thermally-induced wandering of the VLD is analysed. The thermally-induced wandering is most easily characterised by the deviation–deviation correlation function $\langle(h_0-h_r)^2\rangle$, where r is the distance measured parallel to the VLD and h_r is the deviation measured perpendicular to the VLD with respect to a fixed reference. The terms r and h_r are measured in units $2a$ and a, respectively (a is the dimer–dimer distance = 3.84 Å). For a single isolated VLD, the deviation–deviation correlation function $\langle(h_0-h_r)^2\rangle$ diverges linearly with r. This result follows immediately from the random distribution of kinks in the VLD under equilibrium. One can write $\langle(h_0-h_r)^2\rangle=\langle k^2\rangle r$, where $\langle k^2\rangle$ is the mean square displacement of the VLD. When the VLD begin to approach each other, i.e. when the mean square displacement becomes a significant fraction of the VLD–VLD width L, deviations from the linear, "diffusive" behaviour must occur. The repulsive interaction (the leading harmonic term is proportional to σ/L^2) between the VLD results in a flattening out of the deviation–deviation correlation function. For the particular case a formula for the deviation–deviation correlation function has been derived in Ref. [8]:

$$\langle(h_0-h_r)^2\rangle \approx \left(\frac{k_b T\langle k^2\rangle L^2}{2\sigma}\right)^{1/2} \times\left[1-\exp\left(-r\sqrt{\frac{2\sigma\langle k^2\rangle}{k_b TL^2}}\right)\right]. \quad (4)$$

For small r, the linear behaviour, noted earlier, is of course reproduced by Eq. (4). The saturation of $\langle(h_0-h_r)^2\rangle$ with increasing r is clearly an artefact of the fixed-wall approximation (neighbouring VLD are assumed to be fixed walls). One can go beyond the single wandering VLD and let all the VLD wander simultaneously. For large r the deviation–deviation correlation function should diverge. However, this behaviour only becomes important on length scales much larger than the typical VLD–VLD collision distance, i.e. $L^2/\langle k^2\rangle$. By plotting $\langle(h_0-h_r)^2\rangle(L\sqrt{\langle k^2\rangle})^{-1}$ versus $rL^{-1}\sqrt{\langle k^2\rangle}$ a universal curve is found, independent of the actual values of L and $\langle k^2\rangle$. In Fig. 4 a plot of this universal curve (with $\sigma=0.27\pm0.03$ eV/2a) and the experimental data of Ni-induced VLD and Ar-induced VLD is shown. Both types of VLD collapse on the universal curve, indicating that the strength of the long-range interaction is the same and that on length scales up to about the typical VLD–VLD collision length the thermally induced wandering is equilibrated. If there is no dimerisation within the VLD this would imply that $|\sigma_\perp|$ is 3.5 eV/a^2. Even in the absence of a tensile stress component in a direction parallel to the dimer bond, this compressive strain relaxation energy term ($\approx$5–10 meV/a [17]) is not strong enough to compensate for the anisotropy

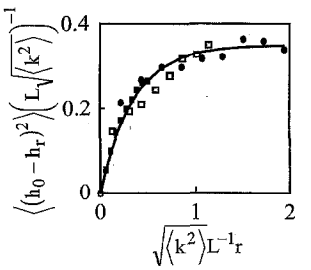

Fig. 4. Scaled mean square displacement of the VLD versus scaled position measured along the VLD. Filled squares and filled circles refer to Ni-induced VLD and open circles refer to Ar^+-induced VLD.

in the island edge formation energy (=34 meV/a [16]) [17]. This result is in agreement with molecular-dynamics calculations performed by Feil et al. [2b], which revealed that the preference of the VLD pattern with respect to the rotated configuration is due to a shorter bonding distance (and hence stronger bonding) between the exposed second-layer atoms and surface atoms at the edges of the VLD.

4. Conclusions

In summary, at low vacancy concentration the VLD pattern is the equilibrium shape, whereas for higher vacancy concentration (>0.2–0.3 monolayers) the equilibrium shape rotates by 90°. The absence of dimerisation within the vacancy island at low vacancy concentration alone cannot explain the preference for the VLD pattern. The formation of the VLD network is driven by a short-range attractive interaction between vacancies in adjacent dimer rows and a long-range repulsive one between vacancies located in the same dimer row. The long-range repulsive interaction is a result of surface strain relaxation and scales as L^{-2}. There are several significant differences between the two types of VLD. First, the Ni-induced VLD cannot be annealed away, whereas the etching-induced VLD can. Second, the etching-induced VLD are one monolayer deep, whereas the Ni-induced ones turn out to be at least two monolayers deep. Third, the Ni-induced VLD network is fully equilibrated, whereas the etching-induced VLD is not fully equilibrated.

References

[1] P. Bedrossian and T. Klitsner, Phys. Rev. Lett. 68 (1992) 646; Phys. Rev. B 44 (1991) 13 783; P. Bedrossian and E. Kaxiras, Phys. Rev. Lett. 70 (1993) 2589.
[2] (a) H.J.W. Zandvliet, H.B. Elswijk, E.J. van Loenen and I.S.T. Tsong, Phys. Rev. B 46 (1992) 7581; (b) H. Feil, H.J.W. Zandvliet, M.-H. Tsai, J.D. Dow and I.S.T. Tsong, Phys. Rev. Lett. 69 (1992) 3076.
[3] P. Bedrossian, Surf. Sci. 301 (1994) 223.
[4] D. Rioux, M. Chander, Y.Z. Li and J.H. Weaver, Phys. Rev. B 49 (1994) 11 071; D. Rioux, R.J. Pechman, M. Chander and J.H. Weaver, Phys. Rev. B 50 (1994) 4430; D. Rioux, F. Stepniak, R.J. Pechman and J.H. Weaver, Phys. Rev. B 51 (1995) 10 981.
[5] K. Wurm, R. Kliese, Y. Hong, B. Röttger, H. Neddermeyer and I.S.T. Tsong, Phys. Rev. B 50 (1994) 1567.
[6] Y. Wei, L. Li and I.S.T. Tsong, Appl. Phys. Lett. 66 (1995) 1818.
[7] N. Kitamura, M.G. Lagally and M.B. Webb, Phys. Rev. Lett. 71 (1993) 2082.
[8] H.J.W. Zandvliet, H.K. Louwsma, P.E. Hegeman and B. Poelsema, Phys. Rev. Lett. 75 (1995) 3890.
[9] H. Niehus, U.K. Köhler, M. Copel and J.E. Demuth, J. Microsc. 152 (1988) 735.
[10] Measuring the depth of such a narrow VLD with STM not only requires a very sharp tip but also electronical effects may play a role.
[11] H. Kahata and K. Yagi, Surf. Sci. 220 (1989) 131.
[12] F.K. Men, A.R. Smith, K.J. Chao, Z. Zhang and C.K. Shih, Phys. Rev. B 52 (1995) 8650.
[13] J.Y. Koo, J.Y. Yi, C. Hwang, D.H. Kim, S. Lee and D.H. Shin, Phys. Rev. B 52 (1995) 17 269.
[14] P. Zeppenfeld, M. Krzyzowski, C. Romainczyk, G. Comsa and M.G. Lagally, Phys. Rev. Lett. 72 (1994) 2737.
[15] N.C. Bartelt, T.L. Einstein and E.D. Williams, Surf. Sci. 276 (1992) 308.
[16] B.S. Swartzentruber et al., Phys. Rev. Lett. 65 (1990) 1913; H.J.W. Zandvliet et al., Phys. Rev. B 45 (1992) 5965.
[17] The island edge formation energies are 60 and 26 meV/a for the S_B and S_A type step edge, respectively. In the absence of a stress component along the dimer direction the strain relaxation energy perpendicular to dimer bond is estimated to be only 6 meV/a ($l=2.5a$ and $L=5.2a$).
[18] V.A. Ukraintsev and J.T. Yates Jr., Surf. Sci. 346 (1996) 31.